Stable and unstable cross-grid P_kQ_l mixed finite elements for the Stokes problem

María G. Armentano [a,*], Jordi Blasco [b]

[a] *Departamento de Matemática, Facultad de Ciencias Exactas y Naturales, Universidad de Buenos Aires, 1428 Buenos Aires, Argentina*
[b] *Departament de Matemàtica Aplicada I, Universitat Politècnica de Catalunya, Campus Sud, Edifici H, Avgda. Diagonal 647, 08028, Barcelona, Spain*

ARTICLE INFO

ABSTRACT

In this paper we develop and analyze a family of mixed finite element methods for the numerical solution of the Stokes problem in two space dimensions. In these schemes, the pressure is interpolated on a mesh of rectangular elements, while the velocity is approximated on a triangular mesh obtained by dividing each rectangle into four triangles by its diagonals. Continuous interpolations of degrees k for the velocity and l for the pressure are considered, so the new finite elements are called cross-grid P_kQ_l. A stability analysis of these approximations is provided, based on the macroelement technique of Stenberg. The lowest order P_1Q_1 and P_2Q_1 cases are analyzed in detail; in the first case, a global spurious pressure mode is shown to exist, so this element is unstable. In the second case, however, stability is rigorously proved. Numerical results obtained in these two cases are also presented, which confirm the existence of the spurious pressure mode for the P_1Q_1 element and the stability of the P_2Q_1 element.

© 2010 Elsevier B.V. All rights reserved.

1. Introduction

In order to approximate the solution of the Stokes problem by finite element methods, there are basically two approaches. The first one consists in approximating the two independent variables, velocity and pressure, using different spaces for each one. This leads to mixed finite element methods, examples of which can be found in [1–8] and in the references therein; mixed methods have been widely analyzed and the theory of mixed problems is well-established nowadays; see [9] (in particular, the paper by D. Boffi, F. Brezzi and M. Fortin, Finite Elements for the Stokes problem on pages 45–100) and [10]. The second approach, which is based on stabilized formulations, consists in modifying the discrete problem by the addition of new terms which enhance its stability (see [11–18] and the references therein).

Both of these approaches have some advantages and some disadvantages. For mixed finite element methods the general theory states that the convergence of these methods is only guaranteed if the discrete spaces are selected such that they satisfy the well-known inf–sup condition (see [9,10]). On the other hand, stabilized methods depend on algorithmic parameters which have to be tuned to get optimal results.

In this work we introduce and analyze a new family of mixed finite element methods in which the pressure is interpolated on a mesh of rectangular elements and the velocity on a triangular mesh obtained by dividing each rectangle into four triangles by its diagonals. The meshing strategy is usually called cross-grid, and similar ideas were employed in [9,10,19,6,7,20,21]. We denote by P_kQ_l the elements in which the velocity is interpolated in each triangle by polynomials of degree no greater than k and the pressure is interpolated in each rectangle by polynomials of degree in each variable no greater than l, with $k \geq l \geq 1$.

---

* Corresponding author.
  E-mail addresses: garmenta@dm.uba.ar (M.G. Armentano), jorge.blasco@upc.edu (J. Blasco).

In order to analyze the stability of these methods, we use the well-known macroelement technique of Stenberg [22–24] which allows us to reduce the analysis of the global stability to a simple local condition. We prove that if the method satisfies a local condition, optimal order of convergence can be obtained. We analyze the lowest order P_1Q_1 element and show the existence of a global spurious pressure mode, so convergence of the pressure does not hold for this element. The alternate nature of the nodal values of the pressure in this spurious mode resembles the structure of the well-known checkerboard mode of the Q_1P_0 element (see for instance [9,25,26]). On the other hand, we prove that the cross-grid P_2Q_1 element satisfies the local estimate and thus the inf–sup condition, so it yields optimally convergent solutions.

Some numerical results are also presented which confirm the presence of the spurious pressure mode for the P_1Q_1 element and the stability of the P_2Q_1 element. Although our methods are introduced and analyzed only in the case of rectangular elements, they can also be appropriately defined in meshes of general quadrilateral elements; we include some numerical experiments on such meshes which show that the nodal checkerboard mode is also present in that case for the P_1Q_1 element, so the presence of this spurious model is not removed by mesh distortion. The P_2Q_1 element, moreover, gives a correct pressure solution and so we conjecture the stability of our cross-grid P_2Q_1 element for general meshes of quadrilateral elements.

The rest of the paper is organized as follows. In Section 2 we state the Stokes problem and introduce the P_kQ_l mixed finite element approximations. In Section 3 we present the stability analysis based on the macroelement technique. In Section 4 we analyze the stability of the lowest order cases P_1Q_1 and P_2Q_1. Finally, in Section 5 we present some numerical examples.

2. Cross-grid P_kQ_l finite element approximation of the Stokes problem

In this section we recall the Stokes problem and we introduce the new family of cross-grid P_kQ_l mixed finite element methods for its numerical approximation.

2.1. Problem statement

Let $\Omega \subset \mathbb{R}^2$ be an open, bounded and polygonal domain. We consider the classical Stokes problem which models the slow motion of an incompressible viscous fluid occupying Ω:

$$\begin{cases} -\mu \Delta \mathbf{u} + \nabla p = \mathbf{f} & \text{in } \Omega, \\ \nabla \cdot \mathbf{u} = 0 & \text{in } \Omega, \\ \mathbf{u} = 0 & \text{on } \Gamma := \partial\Omega, \end{cases} \tag{2.1}$$

where $\mathbf{u}$ is the fluid velocity, p is the pressure, $\mathbf{f} \in (H^{-1}(\Omega))^2$ (the dual space of $(H_0^1(\Omega))^2$) is a given body force per unit mass and $\mu > 0$ is the kinematic viscosity, which we assume constant.

Let $V := (H_0^1(\Omega))^2$ and $Q := L_0^2(\Omega) = \{q \in L^2(\Omega) : \int_\Omega q = 0\}$. The weak form of (2.1) is given by: Find $\mathbf{u} \in V$ and $p \in Q$ such that

$$\begin{cases} a(\mathbf{u}, \mathbf{v}) + b(\mathbf{v}, p) = \langle \mathbf{f}, \mathbf{v} \rangle_{V' \times V} & \forall \mathbf{v} \in V, \\ b(\mathbf{u}, q) = 0 & \forall q \in Q, \end{cases} \tag{2.2}$$

where the bilinear forms $a(\cdot, \cdot)$ and $b(\cdot, \cdot)$ are defined on $V \times V$ and $V \times Q$, respectively, as

$$a(\mathbf{u}, \mathbf{v}) = \mu \int_\Omega \nabla \mathbf{u} : \nabla \mathbf{v} \quad \mathbf{u}, \mathbf{v} \in V,$$

$$b(\mathbf{v}, q) = -\int_\Omega \nabla \cdot \mathbf{v} q \quad \mathbf{v} \in V, q \in Q.$$

The norms and seminorms in $(H^m(D))^2$, with m an integer, are denoted by $\| \cdot \|_{m,D}$ and $| \cdot |_{m,D}$ respectively and $(\cdot, \cdot)_D$ denotes the inner product in $L^2(D)$ or $(L^2(D))^2$ for any subdomain $D \subset \Omega$. The domain subscript is dropped for the case $D = \Omega$.

The bilinear form $a(\cdot, \cdot)$ is coercive in V and there exists a constant $\beta > 0$ (see for instance [9]) such that for all $q \in Q$

$$\sup_{0 \neq \mathbf{v} \in V} \frac{b(\mathbf{v}, q)}{\|\mathbf{v}\|_1} \geq \beta \|q\|_0. \tag{2.3}$$

According to the general theory of mixed problems [9,10] these conditions ensure that there exists a unique solution of problem (2.2).

Let now $V_h \subset V$ and $Q_h \subset Q$ be finite dimensional spaces. The standard Galerkin approximation of (2.2) is given by: Find $(\mathbf{u}_h, p_h) \in V_h \times Q_h$ such that

$$\begin{cases} a(\mathbf{u}_h, \mathbf{v}) + b(\mathbf{v}, p_h) = \langle \mathbf{f}, \mathbf{v} \rangle_{V' \times V} & \forall \mathbf{v} \in V_h, \\ b(\mathbf{u}_h, q) = 0 & \forall q \in Q_h. \end{cases} \tag{2.4}$$

In order to have a stable and convergent approximation, the discrete spaces V_h and Q_h have to satisfy the well-known LBB condition, i.e. there should exist a constant $\tilde{\beta} > 0$, independent of h, such that

$$\sup_{0 \neq \mathbf{v} \in V_h} \frac{b(\mathbf{v}, q)}{\|\mathbf{v}\|_1} \geq \tilde{\beta} \|q\|_0 \quad \forall q \in Q_h. \tag{2.5}$$

Then, if (2.5) holds the theory of mixed finite element methods [9,10] states that problem (2.4) has a unique solution which is stable and optimally convergent, i.e. there exists a positive constant C such that

$$\|\mathbf{u} - \mathbf{u}_h\|_1 + \|p - p_h\|_0 \leq C \{ \inf_{\mathbf{v} \in V_h} \|\mathbf{u} - \mathbf{v}\|_1 + \inf_{q \in Q_h} \|p - q\|_0 \}. \tag{2.6}$$

2.2. Cross-grid $P_k Q_l$ mixed finite elements

We now consider a partition $\mathcal{C}_h$ of $\bar{\Omega}$ into rectangular elements K, which we assume to be regular, i.e. there exists a constant $\sigma > 0$ independent of the mesh size h such that

$$h_K \leq \sigma \rho_K \quad \forall K \in \mathcal{C}_h,$$

where h_K denotes the diameter of K and ρ_K the diameter of the largest ball contained in K.

Then, we divide each rectangle K by its diagonals into four triangles and we call $\mathcal{T}_h$ the resulting mesh of triangular elements T.

Using the standard notation $\mathcal{P}_k$ for the space of polynomials of degree not greater than k and Q_l for the space of polynomials of the form $q(x, y) = \sum_j \alpha_j p_j(x) q_j(y)$ with p_j and q_j polynomials of degree less than or equal to l, the cross-grid $P_k Q_l$ mixed finite element spaces for the approximation of the velocity and the pressure are defined, respectively, as follows:

$$V_h = \{ \mathbf{v} \in V : \mathbf{v}_{|T} \in (\mathcal{P}_k)^2, \ \forall T \in \mathcal{T}_h \}$$

$$Q_h = \{ q \in Q \cap H^1(\Omega) : q_{|K} \in \mathcal{Q}_l, \ \forall K \in \mathcal{C}_h \}.$$

The cases of interest are, of course, those for which $l \leq k$. For $l = k$, we have approximations of the same order for the two variables, although not equal approximations. For $l = k - 1$ the orders of the interpolation errors in the error estimate (2.6) are balanced. Moreover, we are interested in continuous pressure approximations only, so we assume that $l \geq 1$.

3. Stability analysis—The macroelement technique

The goal of this section is to analyze the stability of cross-grid $P_k Q_l$ mixed finite element approximations of the Stokes problem by means of the satisfaction of the discrete inf–sup condition (2.5).

Our stability analysis is based on the well-known macroelement technique of Stenberg (see [22–24]). In the general setting, a macroelement is defined as a connected set M of adjoining (velocity) elements $T \in \mathcal{T}_h$. The macroelement partitioning is called $\mathcal{M}_h$. Two macroelements M and $\bar{M}$ are said to be equivalent if there is a one-to-one and continuous mapping $G : M \to \bar{M}$ such that:

 (i) $G(M) = \bar{M}$.
 (ii) For all $T \subset M$, $G(T) = \bar{T} \subset \bar{M}$.
(iii) For all $T \subset M$, $G_{|T} = F_{\bar{T}} \circ F_T^{-1}$, where F_T and $F_{\bar{T}}$ are affine mappings from the reference element $\tilde{T}$ onto T_j and $\hat{T}$, respectively.

The macroelement partitioning $\mathcal{M}_h$ is usually required to satisfy the following assumptions:

(M1) There is a fixed set of equivalence classes $\mathcal{D}_i$, $i = 1, \ldots, n$, of macroelements such that each $M \in \mathcal{M}_h$ belongs to one of $\mathcal{D}_i$.
(M2) There is a positive integer L such that each $T \in \mathcal{T}_h$ is contained in at least one and not more than L macroelements of $\mathcal{M}_h$.

The cross-grid structure of our velocity mesh $\mathcal{T}_h$ makes the macroelement technique especially suitable for the stability analysis of such elements. The natural choice for macroelements in our case is $M = K$, so the macroelements are indeed the rectangular pressure elements (we use the notation M for the macroelements from now on, rather than using K, since it is standard in this context). Condition (M2) is automatically satisfied with this choice, with $L = 1$. We take the unit square $\hat{M} = [0, 1] \times [0, 1]$ as the reference macroelement. Since in our case every $M \in \mathcal{M}_h$ is a rectangle of the partition $\mathcal{C}_h$, it is clear that there exists an affine transformation F_M such that:

 (i) $F_M(\hat{M}) = M$.
 (ii) If we denote by $\hat{T}_i$, $1 \leq i \leq 4$, the four triangles in $\hat{M}$ obtained by dividing it by its diagonals, then $T_j = F_M(\hat{T}_j)$ are the four triangles of M obtained by dividing it by its diagonals.
(iii) $F_{M_{|\hat{T}_j}} = F_{T_j} \circ F_{\hat{T}_j}^{-1}$, $j = 1, \ldots, 4$, where F_{T_j} and $F_{\hat{T}_j}$ are the mappings from the reference element $\tilde{T}$, i.e. the triangle of vertices $(0, 0)$, $(1, 0)$ and $(0, 1)$, onto T_j and $\hat{T}_j$ respectively.

Thus, all macroelements are equivalent, and condition (M1) is also automatically satisfied, with $n = 1$. For each macroelement M, let us define the following finite element spaces consistent with V_h and Q_h:

$$V_M = \{\mathbf{v} \in (H_0^1(M))^2 : \mathbf{v}_{|T} \in (\mathcal{P}_k)^2, \ \forall T \subset M\}$$
$$Q_M = \mathcal{Q}_l(M).$$

For the elements in Q_M we define the following seminorm:

$$|q|_M = h_M \|\nabla q\|_{0,M}$$

and for $q \in Q_h$ let

$$\|q\|_h^2 = \sum_{M \in \mathcal{C}_h} h_M^2 \|\nabla q\|_{0,M}^2,$$

which can also be written as

$$\|q\|_h^2 = \sum_{M \in \mathcal{C}_h} |q|_M^2.$$

From now on, C denotes a generic positive constant, possibly different at different occurrences, which is independent of h but may depend on the mesh parameter σ and some other parameters introduced in the text.

The following lemmas are the tools for showing that the global stability estimate (2.5) can be obtained from local stability estimates. The proofs follow the same arguments as those given in [22–24]. We have incorporated a modification in the last step of the proof of the following lemma with respect to that of Lemma 1 of [23], and so we give the proof for completeness.

Lemma 3.1. *If there exists a constant C such that for any $M \in \mathcal{C}_h$*

$$\sup_{0 \neq \mathbf{v} \in V_M} \frac{(\nabla \cdot \mathbf{v}, q)_M}{|\mathbf{v}|_{1,M}} \geq C|q|_M \quad \forall q \in Q_M, \tag{3.7}$$

then there exists a constant C such that the following stability inequality holds:

$$\sup_{0 \neq \mathbf{v} \in V_h} \frac{(\nabla \cdot \mathbf{v}, q)}{\|\mathbf{v}\|_1} \geq C\|q\|_h \quad \forall q \in Q_h. \tag{3.8}$$

Proof. Given $q \in Q_h$, the local stability estimate (3.7) implies that for any $M \in \mathcal{C}_h$, there exists $\mathbf{v}_M \in V_M$ such that

$$(\nabla \cdot \mathbf{v}_M, q)_M \geq C|q|_M^2 \tag{3.9}$$

and

$$|\mathbf{v}_M|_{1,M} \leq |q|_M. \tag{3.10}$$

Since $\mathbf{v}_M = 0$ on ∂M, we can define an extension function $\mathbf{v}_M^e \in V_h$ as

$$\mathbf{v}_M^e = \begin{cases} \mathbf{v}_M & \text{in } M \\ 0 & \text{in } \Omega \setminus M. \end{cases}$$

Thus, from (3.9) we have that

$$(\nabla \cdot \mathbf{v}_M^e, q) = (\nabla \cdot \mathbf{v}_M, q)_M \geq C|q|_M^2 \tag{3.11}$$

and from (3.10) we get

$$|\mathbf{v}_M^e|_1 = |\mathbf{v}_M|_{1,M} \leq |q|_M. \tag{3.12}$$

Let us now define

$$\mathbf{v} = \sum_{M \in \mathcal{C}_h} \mathbf{v}_M^e.$$

Then, $\mathbf{v} \in V_h$ and from (3.11) we get

$$(\nabla \cdot \mathbf{v}, q) = \sum_{M \in \mathcal{C}_h} (\nabla \cdot \mathbf{v}_M^e, q) \geq C \sum_{M \in \mathcal{C}_h} |q|_M^2 = C\|q\|_h^2. \tag{3.13}$$

On the other hand, by using the Poincaré inequality and (3.12) we obtain that

$$\|\mathbf{v}\|_1^2 \leq C|\mathbf{v}|_1^2 = C \sum_{M \in \mathcal{C}_h} |\mathbf{v}_M^e|_1^2 \leq C \sum_{M \in \mathcal{C}_h} |q|_M^2 = C\|q\|_h^2. \tag{3.14}$$

Therefore, the lemma follows from (3.13) and (3.14). □

The following lemmas provide a relationship between stability in the mesh-dependent norm $\| \cdot \|_h$ and that in the L^2 norm $\| \cdot \|_0$. The proof of this result is essentially based on the so called Verfurth trick, which was originally used for the proof of stability of Taylor–Hood elements (see [27] and Section 4.3 of [9], *Finite elements for the Stokes problem*). The proof of the next lemma is, thus, skipped.

Lemma 3.2. *There exist two constants C_1 and C_2 such that*

$$\sup_{0 \neq \mathbf{v} \in V_h} \frac{(\nabla \cdot \mathbf{v}, q)}{\|\mathbf{v}\|_1} \geq C_1 \|q\|_0 - C_2 \|q\|_h \quad \forall q \in Q_h.$$

The next lemma is a consequence of Lemma 3.2. Its proof is essentially the same as that of Lemma 3 in [23], and it is therefore omitted.

Lemma 3.3. *If the stability in the mesh-dependent norm (3.8) is valid, then the stability condition (2.5) holds.*

Therefore, the problem of proving that the inf–sup condition (2.5) holds is reduced to proving the local estimates (3.7). In order to get sufficient conditions for these to hold, let us define the space

$$N_M = \{ q \in Q_M | (\nabla q, \mathbf{v})_M = 0, \forall \mathbf{v} \in V_M \}.$$

Since we are in the same conditions as in Lemma 4 of [23], using the same arguments as there, we can prove the following result which gives the fundamental tool for proving the stability of the proposed finite element methods:

Lemma 3.4. *If the space N_M is one-dimensional, i.e., it consists only of functions which are constant on M, then the local stability condition (3.7) holds.*

Combining Lemmas 3.1, 3.3 and 3.4 we obtain the main result of this section:

Theorem 3.1. *If the space N_M is one-dimensional, i.e., it consists only of functions which are constant on M, then the inf–sup condition (2.5) holds, problem (2.4) has a unique solution $(\mathbf{u}_h, p)$ and there exists a constant C independent of the mesh size h such that*

$$\|\mathbf{u} - \mathbf{u}_h\|_1 + \|p - p_h\|_0 \leq C \{ \inf_{\mathbf{v} \in V_h} \|\mathbf{u} - \mathbf{v}\|_1 + \inf_{q \in Q_h} \|p - q\|_0 \}.$$

Remark 3.1. We observe that, under the hypothesis of the previous theorem, if the continuous solution satisfies $\mathbf{u} \in (H^{k+1}(\Omega) \bigcap H_0^1(\Omega))^2$ and $p \in H^{l+1}(\Omega) \bigcap L_0^2(\Omega)$, using classical interpolation error estimates (see for example [28]) we can conclude that $\|\mathbf{u} - \mathbf{u}_h\|_1 + \|p - p_h\|_0 \leq C \{ h^k \|\mathbf{u}\|_{k+1} + h^{l+1} \|p\|_{l+1} \}$.

4. Stability of cross-grid P_kQ_l mixed finite elements

The aim of this section is to analyze the stability of cross-grid P_kQ_l mixed finite elements for different values of k and l, with $k \geq l$ and $l \geq 1$, using the numerical analysis given in Section 3. According to Theorem 3.1, for such elements stability holds if the condition $\dim(N_M) = 1$ is satisfied. Therefore, the following *patch-test* type condition should first be checked if stability is to be expected:

$$\dim V_M \geq \dim Q_M - 1$$

for every macroelement M. Since in our case M is a rectangle of the partition $\mathcal{C}_h$, it is easy to see that for P_kQ_l elements,

$$\dim V_M = 2 \{ 1 + 4(k - 1) + 2(k - 2)(k - 1) \} = 4k^2 - 4k + 2$$
$$\dim Q_M = (l + 1)^2$$

and therefore, P_kQ_l elements satisfy the patch test if

$$4k^2 - 4k + 2 \geq l^2 + 2l.$$

Thus, for the P_kQ_k ($k \geq 1$) mixed interpolations this gives $k > 1.58$, so the lowest order P_1Q_1 element is suspected to be unstable. For the P_kQ_{k-1} ($k \geq 2$) methods, on the other hand, this condition holds for all values of k; the simplest case P_2Q_1 may thus be stable. In the following subsections we consider and analyze in detail the cases P_1Q_1 and P_2Q_1 (see Figs. 1 and 3).
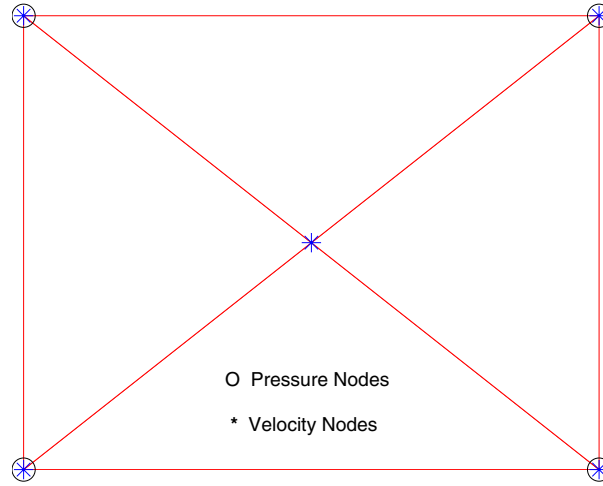
Fig. 1. Velocity and pressure nodes of the cross-grid P_1Q_1 mixed finite element.

4.1. The cross-grid P_1Q_1 element

We first consider the cross-grid P_1Q_1 element, which is the simplest cross-grid element that one can consider among those which use a continuous pressure interpolation. The velocity and pressure nodes of this element are shown in Fig. 1. In this case, $\dim(V_M) = 2$ and $\dim(Q_M) = 4$, so the space N_M is at least two-dimensional. In fact, $\dim(N_M) = 2$ and N_M consists of functions which take the same value at opposite vertices of M. These local spurious pressure modes add up to form a global spurious pressure mode. The next lemma shows the existence of such a pressure mode when Ω is a rectangle and a uniform mesh is considered. Thus, this element does not satisfy the inf–sup condition (2.5).

Lemma 4.1. *Let $\Omega = (0, A) \times (0, B)$ and let $\mathcal{C}_h$ be a uniform mesh consisting of $N \times M$ rectangles. Let us consider the P_1Q_1 mixed finite element approximation. Then, there exists a global spurious pressure mode $\hat{q}_h \in Q_h \setminus \{0\}$ such that*

$$(\nabla \hat{q}_h, \mathbf{v}_h) = 0 \quad \forall \mathbf{v}_h \in V_h.$$

Proof. Let $K_{i,j} = [(i-1)h_x, ih_x] \times [(j-1)h_y, jh_y]$ be the rectangles of the uniform mesh $\mathcal{C}_h$, with $h_x = A/N$, $h_y = B/M$, $1 \le i \le N$ and $1 \le j \le M$, and let $n_{i,j} = (ih_x, jh_y)$, $0 \le i \le N$, $0 \le j \le M$, be the nodes of the mesh $\mathcal{C}_h$. We define $\hat{q}_h \in Q_h$ as

$$\hat{q}_h(n_{i,j}) = \begin{cases} a & \text{if } i+j \text{ is even} \\ -a & \text{if } i+j \text{ is odd} \end{cases}$$

with $a \in \mathbb{R}$, $a \neq 0$. In order to simplify the notation we define $\hat{q}_{i,j} = \hat{q}_h(n_{i,j})$.

Let $p_{i,j}$ be the Lagrange basis of Q_h, i.e. $p_{i,j} \in Q_h$, $p_{i,j}(n_{i,j}) = 1$ and it is zero at the rest of the nodes of the mesh $\mathcal{C}_h$. Then, if $i+j$ is even we have that

$$
\begin{aligned}
\hat{q}_h(x,y)_{|K_{i,j}} &= \hat{q}_{i-1,j-1}p_{i-1,j-1} + \hat{q}_{i,j-1}p_{i,j-1} + \hat{q}_{i-1,j}p_{i-1,j} + \hat{q}_{i,j}p_{i,j} \\
&= a\left(p_{i-1,j-1} + p_{i,j} - p_{i,j-1} - p_{i-1,j}\right) \\
&= a\left\{ \left(\frac{ih_x - x}{h_x}\right)\left(\frac{jh_y - y}{h_y}\right) + \left(\frac{x - (i-1)h_x}{h_x}\right)\left(\frac{y - (j-1)h_y}{h_y}\right) \right. \\
&\quad \left. - \left(\frac{x - (i-1)h_x}{h_x}\right)\left(\frac{jh_y - y}{h_y}\right) - \left(\frac{ih_x - x}{h_x}\right)\left(\frac{y - (j-1)h_y}{h_y}\right) \right\}
\end{aligned}
$$

and so

$$\frac{\partial \hat{q}_h}{\partial x}(x,y)_{|K_{i,j}} = a\left(\frac{y - jh_y}{h_x h_y} + \frac{y - (j-1)h_y}{h_x h_y} - \frac{jh_y - y}{h_x h_y} - \frac{(j-1)h_y - y}{h_x h_y}\right).$$

Let $\mathcal{T}_h$ be the corresponding triangular mesh obtained by dividing each rectangle into four triangles by its diagonals. We denote by $n_{i-1/2,j-1/2} = ((i - 1/2)h_x, (j - 1/2)h_y)$, $1 \le i \le N$, $1 \le j \le M$, the internal node in each rectangle. Let $\beta_{i,j}$ be the piecewise linear Lagrange basis of V_h, i.e., $\beta_{i,j} \in V_h$ such that $\beta_{i,j}(n_{i,j}) = 1$ and it is zero at the rest of the nodes of $\mathcal{T}_h$.
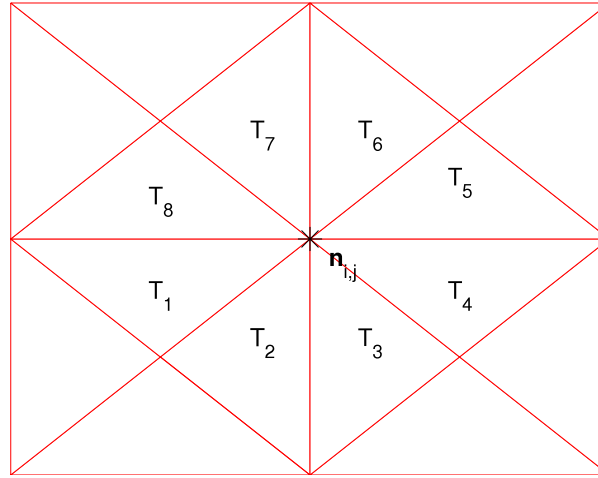
Fig. 2. Support of the shape function $\beta_{i,j}$ for corner nodes $n_{i,j}$.

Let us consider internal nodes $n_{i-1/2,j-1/2}$ first; the support of $\beta_{i-1/2,j-1/2}$ is $K_{i,j}$. Since $\frac{\partial \hat{q}_h}{\partial x}(x, \cdot)_{|K_{i,j}}$ is an odd function with respect to the line $y = (j - 1/2)h_y$ and $\beta_{i-1/2,j-1/2}(x, \cdot)$ is an even function with respect to that line, we conclude that

$$\int_{\Omega} \frac{\partial \hat{q}_h}{\partial x}(x, y)\beta_{i-1/2,j-1/2}(x, y)\mathrm{d}x\mathrm{d}y = \int_{K_{i,j}} \frac{\partial \hat{q}_h}{\partial x}(x, y)\beta_{i-1/2,j-1/2}(x, y)\mathrm{d}x\mathrm{d}y = 0.$$

Now we consider corner nodes $n_{i,j}$ and denote the support of $\beta_{i,j}$ by $w_{i,j} = \cup_{n_{i,j} \in T} T = \cup_{1 \leq l \leq 8} T_l$ (see Fig. 2). An easy calculation shows that

$$\int_{T_l} \frac{\partial \hat{q}_h}{\partial x}(x, y)\beta_{i,j} = -\int_{T_{l+4}} \frac{\partial \hat{q}_h}{\partial x}(x, y)\beta_{i,j} \quad 1 \leq l \leq 4$$

and thus,

$$\int_{\Omega} \frac{\partial \hat{q}_h}{\partial x}(x, y)\beta_{i,j} = \int_{w_{i,j}} \frac{\partial \hat{q}_h}{\partial x}(x, y)\beta_{i,j} = 0.$$

By using the same arguments, we can prove that

$$\int_{\Omega} \frac{\partial \hat{q}_h}{\partial y}(x, y)\beta_{i-1/2,j-1/2}(x, y)\mathrm{d}x\mathrm{d}y = 0$$

and

$$\int_{\Omega} \frac{\partial \hat{q}_h}{\partial y}(x, y)\beta_{i,j}(x, y)\mathrm{d}x\mathrm{d}y = 0.$$

The proof concludes by observing that the case $i + j$ odd is completely analogous and so $(\nabla \hat{q}_h, \mathbf{v}_h) = 0, \forall \mathbf{v}_h \in V_h$. □

Remark 4.1. Due to the alternate nature of the spurious pressure mode $\hat{q}_h$, which resembles the well-known checkerboard mode of the elemental pressures in the $Q_1 P_0$ element, we call this pressure distribution a *nodal checkerboard mode*.

4.2. The cross-grid P_2Q_1 element

We now consider the cross-grid P_2Q_1 element (see Fig. 3). In this case, $\dim(V_M) = 10$ and $\dim(Q_M) = 4$. The following lemma shows that for the P_2Q_1 element the space N_M is one-dimensional and therefore, from Theorem 3.1, we conclude that this element is stable and optimally convergent.

Lemma 4.2. *The space N_M for the cross-grid P_2Q_1 element is one-dimensional.*

Proof. Let $q \in N_M$ be, i.e., $q \in Q_M$ such that $(\nabla q, \mathbf{v})_M = 0 \ \forall \mathbf{v} \in V_M$. We denote by n_j, $1 \leq j \leq 13$, the nodes of the triangulation lying on M and by T_i, $1 \leq i \leq 4$, the triangles in M, as shown in Fig. 4. Let β_j, $1 \leq j \leq 13$, be such that $\beta_{j|_T} \in \mathcal{P}_2$
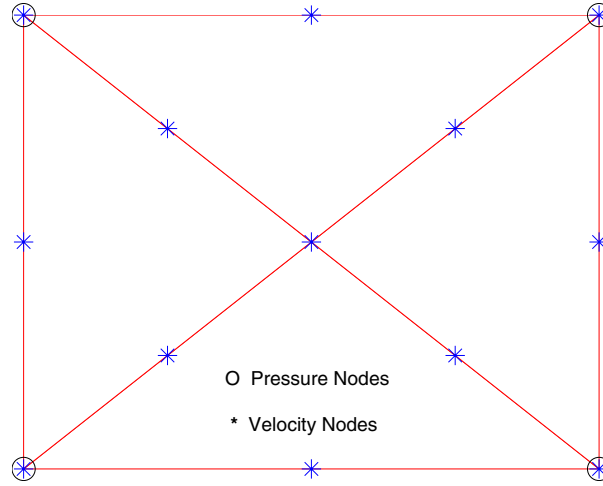
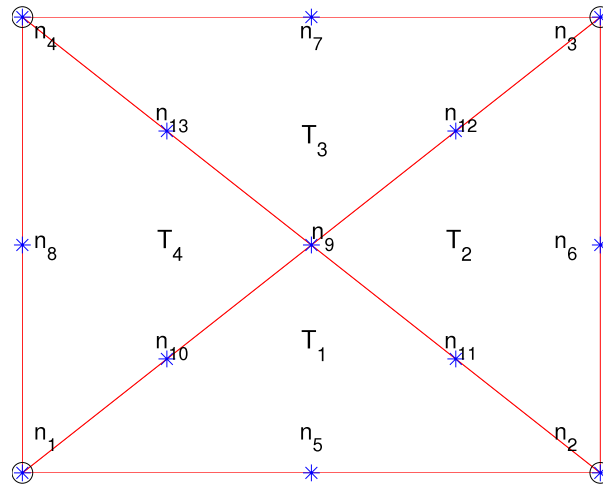**Fig. 3.** Velocity and pressure nodes of the cross-grid P_2Q_1 mixed finite element.

Fig. 4. Local numbering of nodes and triangular elements in the P_2Q_1 case.

and $\beta_j(n_i) = \delta_{i,j}$, i.e. the corresponding $\mathcal{P}_2$-Lagrange basis function of node j. Finally, let p_j, $1 \le j \le 4$, be such that $p_j \in Q_M$ and $p_j(n_i) = \delta_{i,j}$. Then, any $q \in Q_M$ can be written as

$$q(x, y) = \sum_{j=1}^{4} q(n_j) p_j(x, y).$$

We compute explicitly the products $(\nabla q, \mathbf{v})$ for selected velocity fields $\mathbf{v}$. We first notice that these products can be computed on the reference macroelement $\hat{M} = [0, 1] \times [0, 1]$. Indeed, for any macroelement $M \in \mathcal{C}_h$, we have that $\hat{\beta}_j = \beta_j \circ F_M$, $1 \le j \le 13$, and $\hat{p}_i = p_i \circ F_M$, $1 \le i \le 4$, constitute the corresponding Lagrange basis in $\hat{M}$, and from a simple change of variables we get

$$\int_M \frac{\partial p_j}{\partial x}(x, y)\beta_j(x, y)\mathrm{d}x\mathrm{d}y = \int_{\hat{M}} \frac{1}{h_x} \frac{\partial \hat{p}_j}{\partial \hat{x}}(\hat{x}, \hat{y}) \, \hat{\beta}_j(\hat{x}, \hat{y}) h_x h_y \, \mathrm{d}\hat{x}\mathrm{d}\hat{y}$$

$$= h_y \int_{\hat{M}} \frac{\partial \hat{p}_j}{\partial \hat{x}}(\hat{x}, \hat{y}) \hat{\beta}_j(\hat{x}, \hat{y}) \mathrm{d}\hat{x}\mathrm{d}\hat{y},$$

$$\int_M \frac{\partial p_j}{\partial y}(x, y)\beta_j(x, y)\mathrm{d}x\mathrm{d}y = \int_{\hat{M}} \frac{1}{h_y} \frac{\partial \hat{p}_j}{\partial \hat{y}}(\hat{x}, \hat{y}) \, \hat{\beta}_j(\hat{x}, \hat{y}) h_x h_y \, \mathrm{d}\hat{x}\mathrm{d}\hat{y}$$

$$= h_x \int_{\hat{M}} \frac{\partial \hat{p}_j}{\partial \hat{y}}(\hat{x}, \hat{y}) \hat{\beta}_j(\hat{x}, \hat{y}) \mathrm{d}\hat{x}\mathrm{d}\hat{y}$$

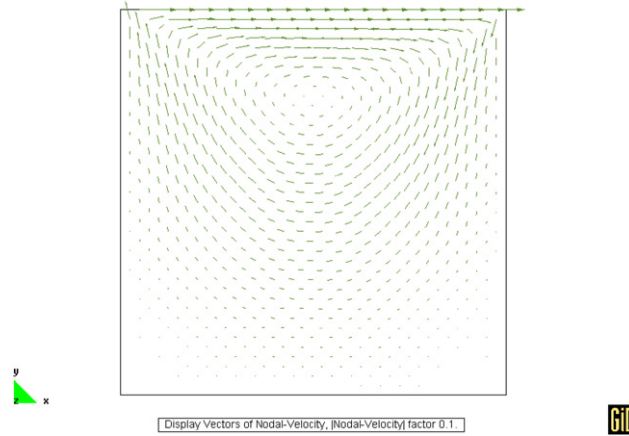where hx and h_y denote the lengths of the edges of M.

Fig. 5. Cavity flow, P_1Q_1 element: Velocity vectors.

Let us first take $\mathbf{v} = (\beta_{10}, 0)$; by the simple calculation of the corresponding integrals we have that condition $(\nabla q, \mathbf{v})_M = 0$ leads to

$$-\frac{7}{60}q(n_1) + \frac{7}{60}q(n_2) + \frac{1}{20}q(n_3) - \frac{1}{20}q(n_4) = 0, \tag{4.15}$$

and taking now $\mathbf{v} = (0, \beta_{10})$ yields

$$-\frac{7}{60}q(n_1) - \frac{1}{20}q(n_2) + \frac{1}{20}q(n_3) + \frac{7}{60}q(n_4) = 0. \tag{4.16}$$

Finally, taking $\mathbf{v} = (0, \beta_{12})$ we obtain

$$-\frac{1}{20}q(n_1) - \frac{7}{60}q(n_2) + \frac{7}{60}q(n_3) + \frac{1}{20}q(n_4) = 0. \tag{4.17}$$

Subtracting (4.16) from (4.15) we get $q(n_2) = q(n_4)$ and adding up (4.15) and (4.17) we get $q(n_1) = q(n_3)$. Substituting these in (4.15) we get $q(n_1) = q(n_2)$, and the proof concludes. □

Remark 4.2. Let us notice that for cross-grid meshes this P_2Q_1 element has the same optimal order of convergence as the well-known P_2P_1 Taylor–Hood element, with the advantage that it requires one less pressure node in each rectangle.

5. Numerical results

We present in this section some numerical results obtained with the P_1Q_1 and the P_2Q_1 cross-grid mixed finite elements on two test cases of the Stokes problem.

5.1. The lid-driven cavity flow problem

In this first example we solved the classical lid-driven cavity flow problem. The fluid domain is the unit square $\Omega = [0, 1] \times [0, 1]$ and the flow is driven by the top lid $\{y = 1, 0 < x < 1\}$, which moves with constant velocity $\mathbf{u} = (1, 0)$; in the rest of the boundary, homogeneous Dirichlet conditions are imposed. Moreover, in this flow problem $\mathbf{f} = 0$, and we took $\nu = 0.1$. In the Stokes case that we consider, the solution to this problem is known to be symmetric about the cavity centerline $x = 0.5$, with a unique primary vortex centered on that line. The pressure is singular at the top corners.

We solved this problem with both the P_1Q_1 and the P_2Q_1 mixed finite elements. In the first case, a uniform mesh of 20×20 rectangular elements was used for the pressure approximation, from which a uniform cross-grid mesh of 1600 triangular elements was generated for the velocity approximation. In the second case, the pressure mesh was courser and consisted only of 10×10 rectangular elements, from which 400 quadratic triangular elements were generated for the velocity. In this way, the number of velocity nodes is the same in the two cases, and equal to 841.

Both elements produced correct velocity solutions, which are plotted in Figs. 5 and 6. As can be observed, both solutions reproduce the main features of the flow such as symmetry and a unique primary vortex.

The pressure solution obtained with the two elements is shown in Figs. 7 and 8 in the form of pressure contours. A clear nodal checkerboard mode phenomenon can be seen in the solution of the P_1Q_1 element, just as predicted by Lemma 4.1.
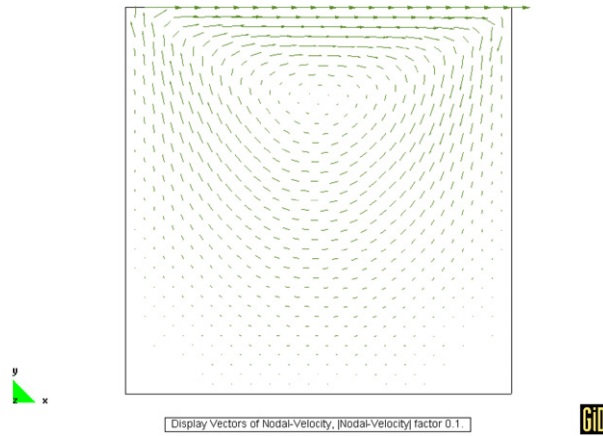
Fig. 6. Cavity flow, $P_2 Q_1$ element: Velocity vectors.
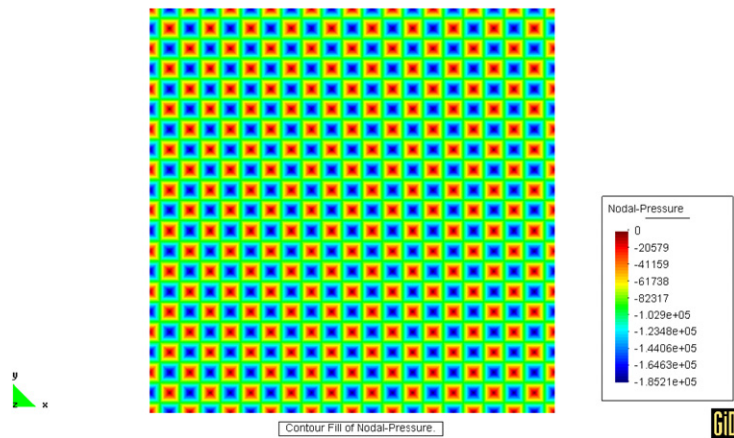
Fig. 7. Cavity flow, $P_1 Q_1$ element: Pressure contours.
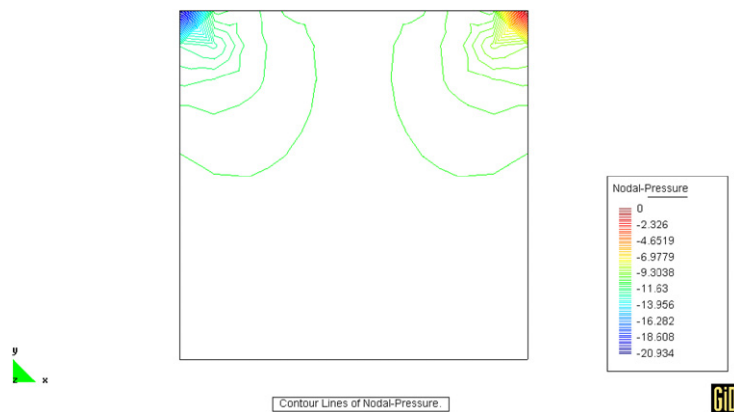
Fig. 8. Cavity flow, $P_2 Q_1$ element: Pressure contours.

The $P_2 Q_1$ element, on the other hand, gave correct pressure results. It has to be said that the hydrostatic (constant) pressure mode was avoided by setting to zero the value of the pressure at the top right corner of the cavity.

Figs. 9 and 10 plot three-dimensional views of the two pressure solutions. The nodal nature of the spurious pressure mode in the $P_1 Q_1$ case can be clearly observed there. In the $P_2 Q_1$ case, on the other hand, the pressure singularity at the top corners is clearly captured.
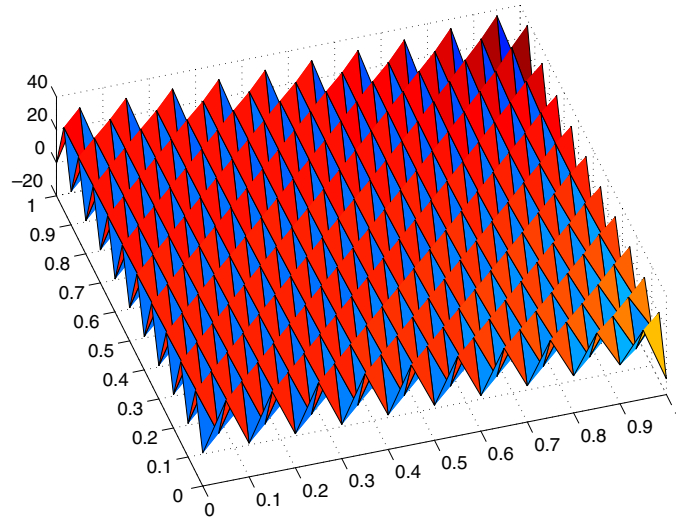
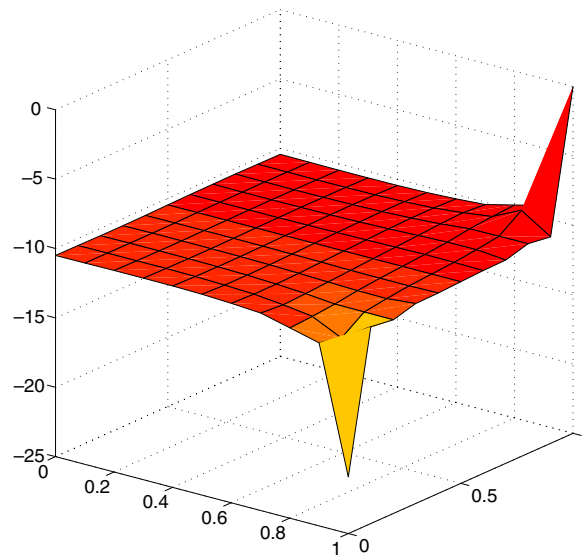**Fig. 9.** Cavity flow, P_1Q_1 element: 3D view of the pressure solution.

Fig. 10. Cavity flow, P_2Q_1 element: 3D view of the pressure solution.

5.2. The trapezoidal domain

Although our cross-grid mixed finite elements have been defined only in the case of meshes of rectangular elements, the methods that we have developed can also be appropriately defined for meshes of regular quadrilateral elements. This second example is intended to test the performance of the P_1Q_1 and the P_2Q_1 elements in such cases.

The problem consists of a fully developed plane Poiseuille flow on a trapezoidal domain of vertices $(0, -1), (5, -1), (2, 1)$ and $(3, 1)$. A parabolic velocity profile is prescribed both at the inlet (left boundary) and at the outlet (right boundary), with a maximum inflow velocity of 1, and a no slip boundary condition is imposed at the top and bottom. The solution of this simple flow problem can introduce some inconsistent boundary conditions on the pressure in some stabilized residual-based formulations (such as GLS) if linear elements are used, which forces the numerical pressure contours to be normal to the boundary (see [29]).

The quadrilateral meshes employed for the pressure approximation in this problem are constructed from 10 (resp. 5) equally spaced subdivisions of each boundary for the P_1Q_1 element (resp. the P_2Q_1 element); the resulting cross-grid triangular meshes can be seen in Fig. 11 for the P_1Q_1 and 12 for the P_2Q_1 element.

The velocity solutions obtained reproduce accurately the analytical solution $\mathbf{u} = (1 - y^2, 0)$ in both cases, and are not plotted. The pressure solutions obtained are shown in Figs. 13 and 14. A nodal checkerboard mode was obtained again with the P_1Q_1 element, so the presence of this spurious model is not removed by mesh distortion. The P_2Q_1 element, on the other
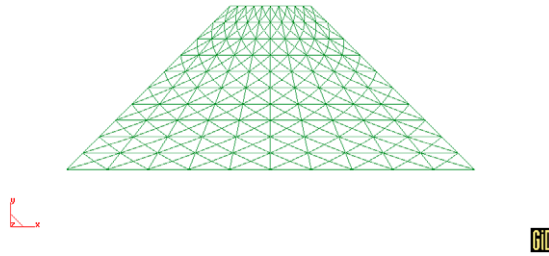
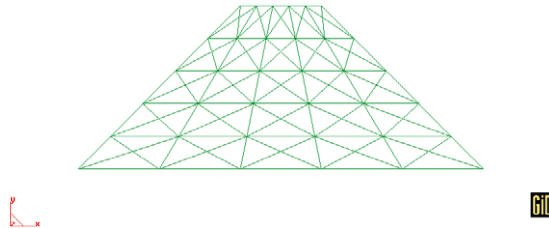**Fig. 11.** Trapezoidal domain, P_1Q_1 element: Velocity mesh.

Fig. 12. Trapezoidal domain, P_2Q_1 element: Velocity mesh.
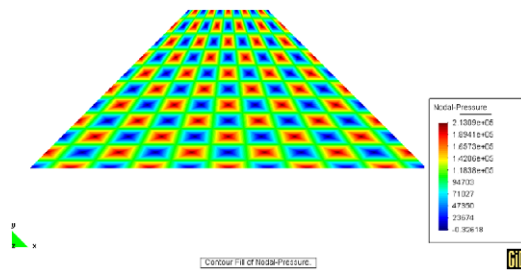

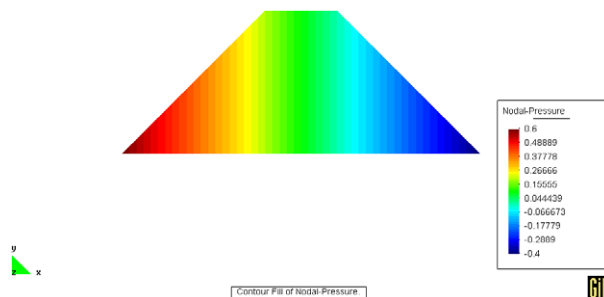**Fig. 13.** Trapezoidal domain, P_1Q_1 element: Pressure contours.

Fig. 14. Trapezoidal domain, P_2Q_1 element: Pressure contours.

hand, gave a correct pressure solution with a linear variation in the x variable, as can be seen in Fig. 14. With this mixed formulation, the pressure is not affected by inconsistent boundary conditions.

Acknowledgements

References

[1] D. Boffi, Minimal stabilizations of the $P_{k+1}-P_k$ approximation of the stationary Stokes equations, Math. J. Models Methods Appl. Sci. 5 (2) (1995) 213–224.

[2] D. Boffi, L. Gastaldi, On the quadrilateral Q_2-P_1 element for the Stokes problem, Int. J. Numer. Methods Fluids 39 (4) (2002) 1001–1011.

[3] F. Brezzi, R. Falk, Stability of higher-order Hood–Taylor methods, SIAM J. Numer. Anal. 28 (3) (1991) 581–590.

[4] X. Chen, W. Han, H. Huang, Analysis of some mixed elements for the Stokes problem, J. Comput. Appl. Math. 85 (1997) 19–35.

[5] M. Fortin, Old and new finite elements for incompressible flows, Int. J. Numer. Methods Fluids 1 (4) (1981) 347–364.

[6] Y. Kim, S. Lee, Stable finite element methods for the stokes problem, Int. J. Math. Math. Sci. 24 (10) (2000) 699–714.

[7] Y. Kim, S. Lee, Modified Mini finite element for the Stokes problem in $\mathbb{R}^2$ or $\mathbb{R}^3$, Adv. Comput. Math. 12 (2000) 261–272.

[8] C. Taylor, P. Hood, A numerical solution of the Navier–Stokes equations using the finite element technique, Int. J. Comput. Fluids 1 (1) (1973) 73–100.

[9] D. Boffi, F. Brezzi, L. Demkowicz, R.G. Durán, R. Falk, M. Fortin, Mixed Finite Elements, Compatibility Conditions, and Applications, in: Lectures Notes in Mathematics, vol. 1939, 2008.

[10] F. Brezzi, M. Fortin, Mixed and Hybrid Finite Element Methods, Springer, Berlin, Heidelberg, New York, 1991.

[11] R. Araya, G.R. Barrenechea, A. Poza, An adaptive stabilized finite element method for the generalized Stokes problem, J. Comput. Appl. Math. 214 (2008) 457–479.

[12] J. Blasco, An anisotropic GLS-stabilized finite element method for incompressible flow problems, Comput. Methods Appl. Mech. Eng. 197 (2008) 3712–3723.

[13] J. Blasco, R. Codina, Space and time error estimates for a first order, pressure stabilized finite element method for the incompressible Navier–Stokes equations, Appl. Numer. Math. 38 (2001) 475–497.

[14] R. Codina, J. Blasco, A finite element formulation for the Stokes problem allowing equal velocity–pressure interpolation, Comput. Methods Appl. Mech. Eng. 143 (3–4) (1997) 373–391.

[15] R. Codina, J. Blasco, Analysis of a pressure-stabilized finite element approximation of the stationary Navier–Stokes equations, Numer. Math. 87 (2000) 59–81.

[16] T.J.R. Hughes, L. Franca, M. Balestra, A new finite element formulation for computational fluid dynamics: V. Circumventing the Babuška–Brezzi condition: A stable Petrov–Galerkin formulation of the Stokes problem accommodating equal order interpolation, Comput. Methods Appl. Mech. Eng. 59 (1) (1986) 85–99.

[17] N. Kechkar, D. Silvester, Analysis of locally stabilized mixed finite element methods for the Stokes problem, Math. Comp. 58 (197) (1992) 1–10.

[18] P. Svácek, On approximation of non-Newtonian fluid flow by the finite element method, J. Comput. Appl. Math. 218 (2008) 167–174.

[19] W. Dahmen, C.A. Micchelli, On the optimal approximation rates for criss-cross finite element spaces, J. Comput. Appl. Math. 10 (3) (1984) 255–273.

[20] Y. Kim, S. Lee, Stable finite element methods with divergence augmentation for the stokes problem, Appl. Math. Lett. 14 (2001) 321–326.

[21] Shi Shu, Jinchao Xu, Ying Yang, Haiyuan Yu, An algebraic multigrid method for finite element systems on criss-cross grids, Adv. Comput. Math. 25 (2006) 287–304.

[22] R. Stenberg, Analysis of Mixed Finite Element Methods for the Stokes problem: A unified approach, Math. Comp. 42 (165) (1984) 9–23.

[23] R. Stenberg, A technique for analysing Finite Element Methods for viscous incompressible fluid flow, Int. J. Numer. Methods Fluids 11 (1990) 935–948.

[24] R. Stenberg, Error analysis of some Finite Element Methods for the Stokes problem, Math. Comp. 54 (190) (1990) 495–508.

[25] R.I. Sani, P.M. Gresho, R.L. Lee, D.F. Griffiths, The cause and cure (?) of the spurious pressures generated by certain FEM solutions of the incompressible Navier–Stokes equations. I, Int. J. Numer. Methods Fluids 1 (1) (1981) 17–43.

[26] R.I. Sani, P.M. Gresho, R.L. Lee, D.F. Griffiths, M. Engelman, The cause and cure (!) of the spurious pressures generated by certain FEM solutions of the incompressible Navier–Stokes equations. II, Int. J. Numer. Methods Fluids 1 (2) (1981) 171–204.

[27] R. Verfurth, Error estimates for a mixed finite element approximation of the Stokes equations, RAIRO Anal. Numer. 18 (2) (1984) 175–182.

[28] S.C. Brenner, L.R. Scott, The Mathematical Theory of Finite Element Methods, Springer-Verlag, New York, 1994.

[29] J.J. Droux, T.J.R. Hughes, A boundary integral modification of the Galerkin least squares formulation for the Stokes problem, Comput. Methods Appl. Mech. Eng. 113 (1994) 173–182.